Modeling and simulation of partially miscible two-phase flow with kinetics mass transfer

Ben Mansour Dia, Bilal Saad, Mazen Saad

Version of Record: https://www.sciencedirect.com/science/article/pii/S0378475420301506
Manuscript_ad83718a88c09d17d13aa1cffef0fa04

Modeling and simulation of partially miscible two-phase flow with kinetics mass transfer

Ben Mansour DIA[a], Bilal SAAD[b], Mazen SAAD[c,*]

[a] *College of Petroleum & Engineering, King Fahd University of Petroleum and Minerals (KFUPM), Dhahran 31261, Saudi Arabia, ben.dia@kfupm.edu.sa*
[b] *Ecole Centrale de Nantes, 1, rue de la Noé 44321 Nantes, France, bilal.saad1984@gmail.com*
[c] *Ecole Centrale de Nantes, Laboratoire de Mathématiques Jean Leray CNRS UMR 6629, 1, rue de la Noé, BP 92101, 44321 Nantes, France*

Abstract

Multiphase flow equations for two components (for instance water and hydrogen) and two phases (liquid and gas), with equilibrium phase exchange, has been used to simulate the process of miscible displacement in porous media. Laboratory and field studies have shown that this assumption fails under certain circumstances especially for accurate description of the pollution and a finite transfer velocity, called here the kinetics. We propose a numerical scheme based on a two-step convection/diffusion-relaxation strategy to simulate the non-equilibrium model. In a first step we solve the intra-phase transfer (convection/diffusion) working with liquid saturation, liquid pressure and dissolved hydrogen concentration as primary variables. In the second step, we address the interphase transfer using the solubility relation that is solved by projection on the equilibrium state. This technique also ensures the positivity for the liquid saturation and produces energy estimates. One important advantage of this approach is the fact that the simulation can be easily adapted to different linear and non-linear equilibrium laws between phases. Another advantage is that our proposed method includes the kinetics in a projection step and keeps the displacement of the components. We implemented this new model in in-house simulation code and present numerical results comparing the model with equilibrium and non-equilibrium one.

Keywords: two-phase, two components, porous media, finite volume, kinetics

1. Introduction

Understanding the transport migration of radionuclides around a nuclear waste repository and its environmental impact is valuable to the study of radioactive waste management that represents a critical issue to tackle for a successful nuclear energy program. In fact, an important quantity of hydrogen can be produced by corrosion of the steel overpack envelope which can affect all the functions allocated to host rock and its safety.
Usually, multiphase flow equations of two components (water and hydrogen) and two phases (liquid and gas) with equilibrium phase exchange, especially the Henry's law, have been used to simulate this process. The local mass equilibrium assumption means that the transfer velocity of a dissolved chemical is infinite. Laboratory and field studies have shown that this assumption fails under certain circumstances especially for accurate description of the pollution and a finite transfer velocity, called here the kinetics. That last seems to give a more accurate description of the pollution [11, 12], [13] or [14].

*Corresponding author
Email address: mazen.saad@ec-nantes.fr (Mazen SAAD)

We propose a numerical scheme based on a two-step convection/diffusion-relaxation strategy to simulate the non equilibrium model. We start by solving the intra-phase transfer (convection/diffusion) working with liquid saturation, liquid pressure and dissolved hydrogen concentration as primary variables. And then, we investigate the interphase transfer using the solubility relation. This technique ensures the validity of the discrete maximum principle for the liquid saturation. Another important advantage of this approach is the fact that the simulation can be easily adapted to different linear and non-linear equilibrium laws between phases. In fact, the first step consists in computing an intermediate solution of mass conservation of each component without the mass transfer terms (kinetic terms). Consequently a various numerical scheme can be used to reach this approximation on several meshes. Then the second step is a simple projection method on the equilibrium state and this step can be modified according to the kinetics.

This paper is organized as follows. In Section 2, we describe the partially miscible two phases two components flows under the assumption of non equilibrium phase exchange and we also recall the two phase two components model when the equilibrium is assumed to satisfy the Henry's law. In Section 3, we present the numerical scheme. For the approximation of the mass conservation system, we detail the construction of a two point flux approximation finite volume scheme. To ensure stability, we use an upstream approach for the mobility of each phase and a non classical mean value of densities. We also describe the projection step. Finally, in Section 4 we compare the solution of our problem with kinetic mass transfer with the results obtained with the equilibrium model. In particular, we compare our results to those proposed by the Benchmak detailed in [17, 3] in which all results are computed with the model with equilibrium.

2. Mathematical formulation of the continuous problem

We consider herein a porous medium saturated with a fluid composed of two phases (liquid and gas) and a mixture of two components (water and hydrogen). The water is supposed to be present in the liquid phase only (no vapor of water due to evaporation). We refer to [3, 18, 6] for more details. Let $T > 0$ be the final fixed time, and Ω be a bounded open subset of $\mathbb{R}^\ell$ ($\ell \geq 1$). We set $Q_T = (0,T)\times\Omega$ with physical boundary $\Sigma_T = (0,T)\times\partial\Omega$. In order to define the physical model, we write the *mass conservation* of each component in each phase

$$(\mathfrak{P})\begin{cases} \partial_t(\Phi\rho_l^w s_l)(t,x) + \mathrm{div}(\rho_l^w \mathbf{V}_l + J_l^w)(t,x) = \overline{\Omega}_l^w, & \text{in } Q_T \\ \partial_t(\Phi\rho_l^h s_l)(t,x) + \mathrm{div}(\rho_l^h \mathbf{V}_l + J_l^h)(t,x) = \overline{\Omega}_l^h, & \text{in } Q_T \\ \partial_t(\Phi\rho_g^h s_g)(t,x) + \mathrm{div}(\rho_g^h \mathbf{V}_g + J_g^h)(t,x) = \overline{\Omega}_g^h, & \text{in } Q_T \\ \partial_t(\Phi\rho_g^w s_g)(t,x) + \mathrm{div}(\rho_g^w \mathbf{V}_g(t,x) + J_g^w)(t,x) = \overline{\Omega}_g^w, & \text{in } Q_T \end{cases}$$

where $\Phi(x)$ is the given porosity of the medium, $s_\alpha(t,x)$ the saturation of the phase α ($\alpha = l,g$) with the saturation condition $s_l + s_g = 1$, ρ_α^β the density of the component β in the phase α, $\rho_\alpha = \rho_\alpha^h + \rho_\alpha^w$ the density of the phase α, $\mathbf{V}_\alpha$ the phase flow velocities, J_α^β the β-component diffusive flux in α phase, and $\overline{\Omega}_\alpha^\beta$ the mass transfer between the components β of each phase α due to chemical reactions and/or phase changes. Note that, as the production of each constituent β in the phase α must be accompanied by destroying this species in the other phase, we have

$$\sum_\alpha \overline{\Omega}_\alpha^h = 0 \quad \text{and} \quad \sum_\alpha \overline{\Omega}_\alpha^w = 0. \tag{1}$$

The velocity of each fluid $\mathbf{V}_\alpha$ is given by the Darcy law

$$\mathbf{V}_\alpha = -\mathbf{K}\frac{k_{r_\alpha}(s_\alpha)}{\mu_\alpha}(\nabla p_\alpha - \rho_\alpha(p_\alpha)\mathbf{g}),$$

where $\mathbf{K}(x)$ is the intrinsic (given) permeability tensor of the porous medium, k_{r_α} the relative permeability of the α phase, μ_α the constant α-phase's viscosity, p_α the α-phase's pressure and $\mathbf{g}$ the gravity. The mobility of each phase is defined as $M_\alpha(s_\alpha) = k_{r_\alpha}(s_\alpha)/\mu_\alpha$.

Following the Fick's law, the diffusive flux of a component β in the phase α is given by

$$J_\alpha^\beta = -\rho_\alpha D_\alpha^\beta \nabla X_\alpha^\beta, \tag{2}$$

where the coefficient D_α^β is the Darcy scale molecular diffusion coefficients of β-component in α-phase and X_α^β is the component β molar fraction in phase α. In a binary system, diffusive fluxes satisfy

$$\sum_\beta J_\alpha^\beta = 0, \quad \forall \alpha. \tag{3}$$

To close the system, we introduce the capillary pressure law which links the jump of pressure of the two phases to the saturation

$$p_c(s_l) = p_g - p_l, \tag{4}$$

the application $s_l \mapsto p_c(s_l)$ is decreasing. This model also corresponds to the application of CO_2 storage when hydrogen is replaced by CO_2.

2.1. Model assuming water incompressibility and no water vaporization

We assume now that the water is incompressible and the water vapor quantity is negligible, i.e., the gas phase contains only hydrogen, then $\rho_g^w = 0,\ p_g^w = 0$. Leading to

$$p_g = p_g^h,\ \rho_g = \rho_g^h,\ J_g^h = J_g^w = 0 \text{ and } \overline{\Omega}_l^w = \overline{\Omega}_g^w = 0. \tag{5}$$

Formulas of $(\mathfrak{P})$ could be rewritten as

$$(\mathfrak{P}) \begin{cases} \partial_t(\Phi\rho_l^w s_l) + \operatorname{div}(\rho_l^w \mathbf{V}_l + J_l^w) = 0, \\ \partial_t(\Phi\rho_g^h s_g) + \operatorname{div}(\rho_g^h \mathbf{V}_g) = \overline{\Omega}_g^h, \\ \partial_t(\Phi\rho_l^h s_l) + \operatorname{div}(\rho_l^h \mathbf{V}_l + J_l^h) = \overline{\Omega}_l^h. \end{cases}$$

2.2. Dynamical phase change between two phases

There are two ways to prescribe the mass transfer between the phases. The first one is to consider a static mass transfer that leads to impose the Henry's law into the system of conservation of the mass of each component [3, 19]. The second approach, used in this paper, is to consider a dynamic mass transfer between gaseous hydrogen and dissolved hydrogen. Dynamic mass transfer means that the equilibrium between the gaseous hydrogen and the dissolved hydrogen is not instantaneous and therefore one has to specify a mass transfer between hydrogen gas and dissolved hydrogen. We prescribe the mass transfer as follows

$$\overline{\Omega}_l^h = -\sigma\rho_l(X_l^h - X_{\text{eq}}),\ \overline{\Omega}_g^h = -\overline{\Omega}_l^h, \tag{6}$$

where σ is the inverse characteristic time to recover the equilibrium between both phases and X_{eq} represents an equilibrium concentration. The system $(\mathfrak{P})$ becomes

$$(\mathfrak{P}) \begin{cases} \partial_t(\Phi\rho_l^w s_l) + \operatorname{div}(\rho_l^w \mathbf{V}_l + J_l^w) = 0, \\ \partial_t(\Phi\rho_g^h s_g) + \operatorname{div}(\rho_g^h \mathbf{V}_g) = \sigma\rho_l(X_l^h - X_{\text{eq}}), \\ \partial_t(\Phi\rho_l^h s_l) + \operatorname{div}(\rho_l^h \mathbf{V}_l + J_l^h) = -\sigma\rho_l(X_l^h - X_{\text{eq}}), \end{cases}$$

which is equivalent to

$$(\mathfrak{P})\begin{cases} \partial_t(\Phi\rho_l^w s_l) - \mathrm{div}(\rho_l^w \mathbf{K} M_l \nabla p_l) + \mathrm{div}(\rho_l D_l^h \nabla X_l^h) = 0, \\ \partial_t(\Phi\rho_g^h s_g) - \mathrm{div}(\rho_g^h \mathbf{K} M_g \nabla p_g) = \sigma\rho_l(X_l^h - X_{\mathrm{eq}}), \\ \partial_t(\Phi\rho_l^h s_l) - \mathrm{div}(\rho_l^h \mathbf{K} M_l \nabla p_l) - \mathrm{div}(\rho_l D_l^h \nabla X_l^h) = -\sigma\rho_l(X_l^h - X_{\mathrm{eq}}). \end{cases}$$

We complete the description of the above model by introducing boundary conditions and initial conditions. We note Γ_l the part the boundary of Ω where the liquid saturation is imposed at given pressure and $\Gamma_n = \Gamma\backslash\Gamma_l$ the part of the boundary with no fluxes. The chosen mixed boundary conditions on the pressures are

$$\begin{cases} p_l(t,x) = p_g(t,x) = 0 & \text{on } (0,T)\times\Gamma_l, \\ \mathbf{K}M_l\nabla p_l\cdot\mathbf{n} = \mathbf{K}M_g\nabla p_g\cdot\mathbf{n} = D_l^h\nabla X_l^h\cdot\mathbf{n} & \text{on } (0,T)\times\Gamma_n = 0. \end{cases} \tag{7}$$

The initial conditions are defined on pressures

$$p_\alpha(0,x) = p_\alpha^0(x), \text{ in } \Omega, \text{ for } \alpha = l,g. \tag{8}$$

We call this system, DYNMOD "DYNamical Mass transfert mODel". In [21] the authors propose a numerical scheme to solve the system and they consider the velocity σ as a given function but numerical experiments were not performed due to the lack of data for the velocity. Our aim here is to propose a numerical scheme for which this difficulty is to overcome the lack of data by using a projection step on the equilibrium state. We elaborate our method in the next section.

In order to compare the two models, we recall here the system with equilibrium (see [6, 19]). We write the *mass conservation* of each component in Q_T

$$\begin{cases} \partial_t(\Phi s_l\rho_l^h + \Phi s_g\rho_g^h) + \mathrm{div}(\rho_l^h\mathbf{V}_l + \rho_g^h\mathbf{V}_g) - \mathrm{div}(\rho_l D_l^h\nabla X_l^h) = 0, & (9) \\ \partial_t(\Phi s_l\rho_l^w) + \mathrm{div}(\rho_l^w\mathbf{V}_l) = 0. & (10) \end{cases}$$

We complete this system by the same boundary and initial conditions (7) and (8).
To define the hydrogen densities, we use the ideal gas law and the Henry law

$$\rho_g^h = \frac{M^h}{RT}p_g,\ \rho_l^h = M^h H^h p_g, \tag{11}$$

where the quantities M^h, H^h, R and T represent respectively the molar mass of hydrogen, the Henry constant for hydrogen, the universal constant of perfect gases and T the temperature. From (11), we get

$$\rho_g^h = C_1\rho_l^h \text{ where } C_1 = \frac{1}{H_h RT}(= 52.51). \tag{12}$$

In the sequel, we call the system (9)–(10) HELMOD " Henry's Law MODel".

3. Numerical Scheme

We propose a numerical scheme based on a two-step convection/diffusion-relaxation strategy to simulate the non equilibrium model. In a first step we solve the intra-phase transfer (convection/diffusion) working with liquid saturation, liquid pressure and dissolved hydrogen concentration as primary variables. The second step solves the interphase transfer, using the solubility relation.

In the following, firstly we describe the semi discretization in time of the numerical method and next we detail the discretization in space.

Consider $U^n = ((s_l)^n,(p_l)^n,(\rho_l^h)^n)$ is given at time t^n, then to compute the solution at the next time step $U^{n+1} = ((s_l)^{n+1},(p_l)^{n+1},(\rho_l^h)^{n+1})$, we consider an intermediate solution, named $U^* = ((s_l)^*,(p_l)^*,(\rho_l^h)^*)$, of the system $(\mathfrak{P})$ without the reaction terms

$$\begin{cases} \partial_t(\Phi\rho_l^w s_l) + \mathrm{div}(\rho_l^w \mathbf{V}_l + J_l^w) = 0, & (13)\\ \partial_t(\Phi\rho_g^h s_g) + \mathrm{div}(\rho_g^h \mathbf{V}_g) = 0, & (14)\\ \partial_t(\Phi\rho_l^h s_l) + \mathrm{div}(\rho_l^h \mathbf{V}_l + J_l^h) = 0. & (15) \end{cases}$$

The approximation of the solution of the above system is detailed in section 3.1. Then, the second step to compute $U^{n+1} = ((s_l)^{n+1},(p_l)^{n+1},(\rho_l^h)^{n+1})$ is to ensure the equilibrium when the σ goes to infinity which gives $\{X_l^h = X_{\mathrm{eq}}\}$, and leads to the following state :

$$\begin{cases} \partial_t(\rho_l^w s_l) = 0 \\ \partial_t(\rho_g^h s_g + \rho_l^h s_l) = 0 \end{cases} \tag{16}$$

In section 3.2, we detail this projection step.

In the sequel, we consider an isotropic medium, and we set $\mathbf{K} = kI_d$, where I_d is the identity matrix.

3.1. Step 1. The TPFA scheme to solve system (13)–(15)

In this section, we detail the construction of the Two Point Flux Approximation (TPFA) scheme based on upstream approximation of mobilities according to the sign of the pressure of each phase at the interfaces of mesh and on a specific choice of densities on the mesh interfaces. We will describe the space and time discretization, define the approximation spaces, and introduce the finite volume scheme.

3.1.1. The orthogonal mesh

Following [7] and [2], let us specify a finite volume discretization of $\Omega\times(0,T)$.

Definition 3.1. *(**Admissible mesh of** Ω). An admissible mesh $\mathcal{T}$ of Ω is given by a set of open bounded polygonal convex subsets of Ω called control volumes and a family of points (the "centers" of control volumes) satisfying the following properties:*

1. *The closure of the union of all control volumes is $\overline{\Omega}$. We denote by $|K|$ the measure of K, and define size$(\mathcal{T}) = max\{diam(K), K \in \mathcal{T}\}$.*
2. *For any $(K,L) \in \mathcal{T}^2$ with $K \neq L$, then $K \cap L = \emptyset$. One denotes by $\mathcal{E} \subset \mathcal{T}^2$ the set of (K,L) such that the $(\ell-1)$-Lebesgue measure of $\overline{K} \cap \overline{L}$ is positive. For $(K,L) \in \mathcal{E}$, one denotes $\sigma_{K|L} = \overline{K} \cap \overline{L}$ and $|\sigma_{K|L}|$ the $(\ell-1)$-Lebesgue measure of $\sigma_{K|L}$. And one denotes $\eta_{K|L}$ the unit normal vector to $\sigma_{K|L}$ outward to K*
3. *For any $K \in \mathcal{T}$, one defines $N(K) = \{L \in \mathcal{T}, (K,L) \in \mathcal{E}\}$ and one assumes that $\partial K = \overline{K}\backslash K = (\overline{K} \cap \partial\Omega) \cup (\cup_{L\in N(K)} \sigma_{K|L})$.*
4. *The family of points $(x_K)_{K\in\mathcal{T}}$ is such that $x_K \in K$ (for all $K \in \mathcal{T}$) and, if $L \in N(K)$, it is assumed that the straight line (x_K, x_L) is orthogonal to $\sigma_{K|L}$. We set $d_{K|L} = d(x_K, x_L)$ the distance between the points x_K and x_L, and $\tau_{K|L} = \frac{|\sigma_{K|L}|}{d_{K|L}}$ the transmissibility coefficient through $\sigma_{K|L}$ (see Figure 1).*
5. *We assume the following regularity of the mesh : there exists $\xi > 0$, such that*

$$\forall K \in \mathcal{T}, \sum_{L\in N(K)} |\sigma_{K|L}| d_{K|L} \leq \xi |K|.$$

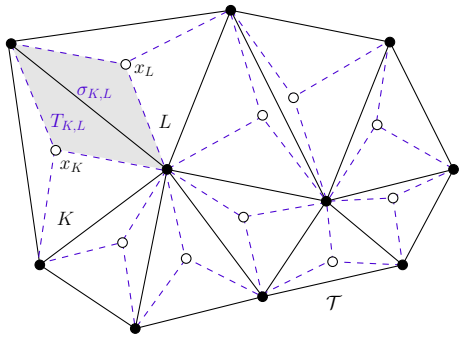

Figure 1: Finite volume mesh $\mathcal{T}$: control volumes, centers and diamonds.

Discrete functions and notations. The problem under consideration is time-dependent, the time discretization of $(0,T)$ is given by an integer value N and a uniform time step $\delta t = T/(N+1)$, we denote $(t^n = n\delta t)_{n\in[0,N+1]}$ with $t^0 = 0$ and $t^{N+1} = T$. Let $\mathcal{T}_{\delta t}$ be a discretization of Q_T. We denote any function u from $[0,N+1]\times\mathcal{T}$ to $\mathbb{R}$ by using the subscript $\mathcal{T}_{\delta t}$ and we denote its value at the point (t_n,x_K) as u_K^n, we then denote $u_{\mathcal{T}_{\delta t}} = (u_K^n)_{K\in\mathcal{T},n\in[0,N+1]}$. To any discrete function $u_{\mathcal{T}_{\delta t}}$ corresponds an approximate function defined almost everywhere on Q_T by:

$$u_{\mathcal{T}_{\delta t}}(t,x) = u_K^{n+1}, \text{ for a.e. } (t,x)\in(t^n,t^{n+1})\times K, \forall K\in\mathcal{T}, \forall n\in[0,N].$$

In the same way, we denote the discrete function $u_{\mathcal{T}}^{n+1}$ defined from $\mathcal{T}$ to $\mathbb{R}$ associated to the vector $(u_K^{n+1})_{K\in\mathcal{T}}$ as

$$u_{\mathcal{T}}^{n+1}(x) = u_K^{n+1}, \text{ for a.e. } x\in K, \forall K\in\mathcal{T}.$$

The discrete gradient. For each interface $\sigma_{K|L}$, we associate a diamond $T_{K|L}$ when the two elements K and L exist by connecting the vertices of interface and the centers of K and L, and in the case where the interface lies on $\partial\Omega$, we associate a half of diamond denoted $T_{K|\sigma}^{\text{ext}}$ associated to the element K with $\sigma\subset\partial\Omega$.
For each discrete function $u_{\mathcal{T}}^{n+1} = (u_K^{n+1})_{K\in\mathcal{T}}$, we associate $\nabla_{\mathcal{D}}u_{\mathcal{T}}^{n+1}$, $\mathbb{R}^\ell$-valued function, defined on the dual mesh as the constant per diamond

$$\nabla_{\mathcal{D}}u_{\mathcal{T}}^{n+1}(x) = \begin{cases} \ell\frac{u_L-u_K}{d_{K|L}}\eta_{K|L} \text{ if } x\in T_{K|L}, \\ \\ \ell\frac{u_\sigma-u_K}{d_{K,\sigma}}\eta_{K|\sigma} \text{ if } x\in T_{K|\sigma}^{\text{ext}}. \end{cases}$$

To take into account the no flux boundary we impose $u_\sigma = u_K$ and for imposing pressure or saturation, we consider u_σ to be the given value at the boundary.
For any discrete function defined on diamonds $u_{\mathcal{D}}^{n+1} = (u_{K|L}^{n+1})_{\sigma_{K|L}\in\mathcal{E}}$ corresponds to

$$u_{\mathcal{D}}^{n+1}(x) = u_{K|L}^{n+1}, \text{ for a.e. } x\in T_{K|L}. \tag{17}$$

3.1.2. The coupled finite volume scheme

The finite volume scheme consists in writing the balance equations of the fluxes on each control volume. Let $\mathcal{T}_{\delta t}$ be a discretization of $\Omega\times(0,T)$. Let us integrate the liquid saturation equation (13), the hydrogen in the gaseous form (14) and dissolved hydrogen concentration (15) over each control volume K.

For clarity and simplicity, we restrict the theoretical demonstration to a horizontal field, i.e. we neglect the gravity effect. The resulting equation is discretized with an implicit Euler scheme in time; the normal gradients across the interfaces are discretized with a centered finite difference scheme whereas the mobilities are approximated with an upwind scheme.

Denote by $s_{l,\mathcal{T}_{\delta t}} = (s^n_{l,K})_{K\in\mathcal{T},n\in[0,N+1]}$, $p_{l,\mathcal{T}_{\delta t}} = (p^n_{l,K})_{K\in\mathcal{T},n\in[0,N+1]}$ and $\rho^h_{l,\mathcal{T}_{\delta t}} = (\rho^{h,n}_{l,K})_{K\in\mathcal{T},n\in[0,N+1]}$ the discrete unknowns corresponding to s_l, p_l, ρ^h_l. The finite volume scheme is the following set of equations :

$$q^0_K = \frac{1}{|K|}\int_K q^0(x)\mathrm{d}x, \text{ for all } K\in\mathcal{T}, \text{ and } q = s_l, p_l, \rho^h_l \tag{18}$$

For $n = 0,\ N$

$$|K|\,\Phi_K\rho^w_l\frac{s^{n+1}_{l,K}-s^n_{l,K}}{\delta t} - \sum_{L\in N(K)}\tau_{K|L}\rho^w_l M^{n+1}_{l,K|L}(p^{n+1}_{l,L}-p^{n+1}_{l,K}) + \sum_{L\in N(K)}\tau_{K|L}\rho^{n+1}_{l,K|L}D^{h,n+1}_{l,K|L}(X^{h,n+1}_{l,L}-X^{h,n+1}_{l,K}) = 0 \tag{19}$$

$$|K|\,\Phi_K\frac{\rho^{h,n+1}_{g,K}s^{n+1}_{g,K}-\rho^{h,n}_{g,K}s^n_{g,K}}{\delta t} - \sum_{L\in N(K)}\tau_{K|L}\rho^{n+1}_{g,K|L}M^{n+1}_{g,K|L}(p^{n+1}_{g,L}-p^{n+1}_{g,K}) = 0 \tag{20}$$

$$|K|\,\Phi_K\frac{\rho^{h,n+1}_{l,K}s^{n+1}_{l,K}-\rho^{h,n}_{l,K}s^n_{l,K}}{\delta t} - \sum_{L\in N(K)}\tau_{K|L}\rho^{h,n+1}_{l,K|L}M^{n+1}_{l,K|L}(p^{n+1}_{l,L}-p^{n+1}_{l,K}) - \sum_{L\in N(K)}\tau_{K|L}\rho^{n+1}_{l,K|L}D^{h,n+1}_{l,K|L}(X^{h,n+1}_{l,L}-X^{h,n+1}_{l,K}) = 0 \tag{21}$$

The mean value of the densities of each phase on interfaces is not classical since it is given as, for all function $\rho(p) = \rho_l(p_l)$, $\rho^h_g(p_g)$, and $\rho^h_l(p_l)$ as

$$\frac{1}{\rho^{n+1}_{K|L}} = \begin{cases} \frac{1}{p^{n+1}_L-p^{n+1}_K}\int_{p^{n+1}_K}^{p^{n+1}_L}\frac{1}{\rho(\zeta)}\,d\zeta & \text{if } p^{n+1}_K\neq p^{n+1}_L,\\ \frac{1}{\rho^{n+1}_K} & \text{otherwise,}\end{cases} \tag{22}$$

and where $M^{n+1}_{\alpha,K|L} = M_\alpha(s^{n+1}_{\alpha K|L})$ denotes the upwind approximation of the mobility on the interface $\sigma_{K|L}$ with

$$s^{n+1}_{\alpha,K|L} = \begin{cases} s^{n+1}_{\alpha,K} & \text{if } p^{n+1}_{\alpha,K}\geq p^{n+1}_{\alpha,L},\\ s^{n+1}_{\alpha,L} & \text{otherwise.}\end{cases} \tag{23}$$

This choice is crucial to obtain estimates on discrete global pressure and on saturation.

This scheme consists in a two point flux approximation finite volume method together with a phase-by-phase upstream scheme and a nonclassical mean value for densities. The Euler implicit discretization

in time and the proposed finite volume scheme satisfy industrial constraints of robustness and stability. In comparison with incompressible fluid, compressible fluids require more powerful techniques. The treatment of the degeneracy and the nonlinearly need the introduction of powerful techniques to link the velocities to the global pressure and the capillary pressure on the discrete form, we refer to [21, 2, 6].

Proposition 3.1. *The finite volume scheme* (19)–(21) *is equivalent to the variational discrete formulation:*

$$\begin{aligned}\int_\Omega \Phi_\mathcal{T}\rho_l^w \frac{s_{l,\mathcal{T}}^{n+1}-s_{l,\mathcal{T}}^{n}}{\delta t}\varphi_\mathcal{T}^{n+1}\,dx \quad &+ \quad \frac{1}{\ell}\int_\Omega \rho_l^w M_{l,\mathcal{D}}^{n+1}\nabla_\mathcal{T} p_{l,\mathcal{T}}^{n+1}\cdot\nabla_\mathcal{D}\varphi_\mathcal{T}^{n+1}\,dx \\ &- \quad \frac{1}{\ell}\int_\Omega \rho_{l,\mathcal{D}}^{n+1} D_{l,\mathcal{D}}^{h,n+1}\nabla_\mathcal{D} X_{l,\mathcal{T}}^{h,n+1}\cdot\nabla_\mathcal{D}\varphi_\mathcal{T}^{n+1}\,dx \;=0\end{aligned} \tag{24}$$

$$\begin{aligned}\int_\Omega \Phi_\mathcal{T}\frac{\rho_{g,\mathcal{T}}^{h,n+1}s_{g,\mathcal{T}}^{n+1}-\rho_{g,\mathcal{T}}^{h,n}s_{g,\mathcal{T}}^{n}}{\delta t}\xi_\mathcal{T}^{n+1}\,dx \\ +\frac{1}{\ell}\int_\Omega \rho_{g,\mathcal{D}}^{h,n+1}M_{g,\mathcal{D}}^{n+1}\nabla_\mathcal{D} p_{g,\mathcal{T}}^{n+1}\cdot\nabla_\mathcal{D}\xi_\mathcal{T}^{n+1}\,dx=0\end{aligned} \tag{25}$$

$$\begin{aligned}\int_\Omega \Phi_\mathcal{T}\frac{\rho_{l,\mathcal{T}}^{h,n+1}s_{l,\mathcal{T}}^{n+1}-\rho_{l,\mathcal{T}}^{h,n}s_{l,\mathcal{T}}^{n}}{\delta t}\psi_\mathcal{T}^{n+1}\,dx+\frac{1}{\ell}\int_\Omega \rho_{l,\mathcal{D}}^{h,n+1}M_{l,\mathcal{D}}^{n+1}\nabla_\mathcal{D} p_{l,\mathcal{T}}^{n+1}\cdot\nabla_\mathcal{D}\psi_\mathcal{T}^{n+1}\,dx \\ +\frac{1}{\ell}\int_\Omega \rho_{l,\mathcal{D}}^{n+1}D_{l,\mathcal{D}}^{h,n+1}\nabla_\mathcal{D} X_{l,\mathcal{T}}^{h,n+1}\cdot\nabla_\mathcal{D}\psi_\mathcal{T}^{n+1}\,dx \;=0\end{aligned} \tag{26}$$

for all $\varphi_\mathcal{T}$, $\xi_\mathcal{T}$, $\psi_\mathcal{T}\in H_h$, *where the function* $M_{l,\mathcal{D}}^{n+1}$, $M_{g,\mathcal{D}}^{n+1}$, $M_\mathcal{D}^{n+1}$ *are defined to be constant by diamonds as in* (17).

Proof. Multiply the equations (19), (20), and (21) respectively by φ_K, ξ_K and ψ_K and sum over all $K\in\mathcal{T}$, then integrating by parts we obtain (24), (25) and (26)

We summarize the main energy estimates on the problem :

Proposition 3.2 (Maximum principle). *Let* $(s_{\alpha,K}^0)_{K\in\mathcal{T}}\in[0,1]$. *Then, the saturation* $(s_{l,K}^n)_{K\in\mathcal{T},n\in\{0,\dots,N\}}$ *is nonnegative.*

Proposition 3.3 (Energy estimates). *The solution of the TPFA scheme satisfies*

$$\sum_{n=0}^{N}\int_\Omega\left(M_{l,\mathcal{D}}^{n+1}|\nabla_\mathcal{T} p_{l,\mathcal{T}}^{n+1}|^2+M_{g,\mathcal{D}}^{n+1}|\nabla_\mathcal{T} p_{g,\mathcal{T}}^{n+1}|^2\right)dx\le C, \tag{27}$$

Proof. We give here some elements of the proof and we refer to [21, 20]. To prove the estimate (27), we consider in (24) the test function $C_1 p_{l,\mathcal{T}}^{n+1}-p_{g,\mathcal{T}}^{n+1}$, where C_1 is defined in (12), and in equations (25)–(26) we take the nonlinear test function $g_g(p_{g,K}^{n+1})=\int_0^{p_{g,K}^{n+1}}\frac{1}{\rho_l^h(z)}\mathrm{d}z$, then summing the resulting equation to deduce the estimates on velocities.

3.2. Step 2. Projection at equilibrium state

In the following, we describe the second step, called projection (relaxation) step, of the numerical method to simulate ($\mathfrak{P}$).

In the first step, using the finite volume TPFA scheme (19)–(21) to solve the mass conservation system ($\mathfrak{P}$) without the source term, gives from $U_K^n = ((s_l)_K^n,(p_l)_K^n,(\rho_l^h)_K^n)$ an intermediate state $U_K^* = ((s_l)_K^*,(p_l)_K^*,(\rho_l^h)_K^*)$. Formally, as σ tends to $+\infty$, which is to look for U_K^{n+1} solution of $\{X_l^h = X_{\text{eq}}\}$. Remark that as σ is finite, we have the conservation of mass

$$\begin{cases} \partial_t(\rho_l^w s_l) = 0 \\ \partial_t(\rho_g^h s_g + \rho_l^h s_l) = 0 \end{cases} \tag{28}$$

at the discrete level . As ρ_l^w is constant, the first equation gives $(s_l)_K^{n+1} = (s_l)_K^*$. Define $\rho^h = \rho_g^h s_g + \rho_l^h s_l$, the second equation imposes

$$(U)_K^{n+1} + (V)_K^{n+1} = (\rho^h)_K^*, \qquad \forall K \in \mathcal{T}, \tag{29}$$

where $U = \rho_g^h s_g$, $V = \rho_l^h s_l$ and $(\rho^h)_K^* = (\rho_g^h s_g + \rho_l^h s_l)_K^*$ which can be computed from $(s_l)_i^*$, $(p_l)_i^*$ and $(\rho_l^h)_i^*$.

From the Henry's law that connects s_l, p_l and ρ_l^h

$$M^h H(T) p_g - \rho_l^h = 0, \tag{30}$$

we have the following:

$$s_l H^h RTU - s_g V = 0.$$

Considering the above equality at time t^{n+1} and for all K, one gets

$$(s_l)_K^{n+1} H^h RTU_K^{n+1} - (s_g)_K^{n+1} V_K^{n+1} = (s_l)_K^* H^h RTU_K^{n+1} - (s_g)_K^* V_K^{n+1} = 0$$

that gives by using (29), the following relation

$$V_K^{n+1} = \frac{(s_l)_K^*\, H^h RT(\rho^h)^*}{(s_g)_K^* + (s_l)_K^*\, H^h RT}. \tag{31}$$

Then, from V_K^{n+1} we can compute $(\rho_l^h)_K^{n+1}$, using (29) we can compute U_K^{n+1} and consequently $p_{l,K}^{n+1}$.

4. Numerical results: Gas phase (dis)appearance (quasi-1D)

In this section, we evaluate numerically the numerical scheme derived in the above section on a test case dedicated to gas-phase (dis)appearance(see the Couplex-Gas benchmark [17, 4] for more details). The method has been implemented into in-house code.

In order to investigate numerically the phenomena of the evolution of an non-equilibrium state to a stabilized one, which stands to be a particular case of the configuration where a non saturated porous block is placed within a water saturated porous structure, we consider a sealed porous medium. In this numerical test, we intend to describe the recovery of the mechanical balance in a porous medium that is initially out of the equilibrium. The initial non-equilibrium is characterized with the occurrence of jumps in the phase pressures, which are typically noticed when the engineered barriers are set quite close to the waste packages.

Let Ω be the porous medium which contains subdomains Ω_1 and Ω_2. The porous medium is considered to be homogeneous and sealed core, thus we impose no fluxes boundary on $\partial\Omega$. The length of Ω is $L_x = 1m$ and the length of Ω_1 is $L_1 = 0.5m$ and the width of Ω is $L_y = 0.1m$ see figure 2.

The porous medium and fluid characteristics are presented in [17] and summarized in Table 1.

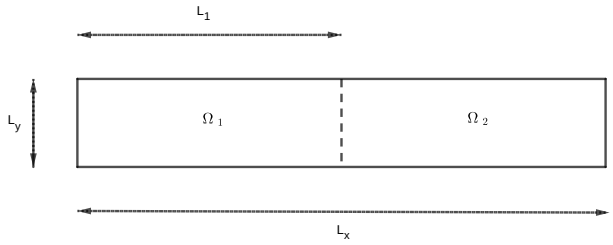

Figure 2: Geometrical configuration of the domain

Porous medium		**Fluid characteristics**	
Parameter	*Value*	*Parameter*	*Value*
Φ [-]	0.3	D_l^h [$m^2 \cdot s^{-1}$]	3×10^{-9}
$\mathbf{K}$ [m^2]	1.10^{-16}	μ_l [$Pa \cdot s$]	1×10^{-3}
p_r [Pa]	2×10^6	μ_g [$Pa \cdot s$]	9×10^{-6}
n [-]	1.54	H^h [$mol.Pa^{-1}.m^{-3}$]	7.65×10^{-6}
s_{lr} [-]	0.01	M^h [$Kg \cdot mol^{-1}$]	2×10^{-3}
s_{gr} [-]	0	ρ_l^w [$Kg \cdot mol^{-3}$]	10^3

Table 1: Parameter values for the porous medium and fluid characteristics used in this test

The initial conditions are given as follows

$$p_l = 10^6 \text{ Pa and } p_g = 1.5\times10^6 \text{ Pa in } \Omega_1,$$
$$p_l = 10^6 \text{ Pa and } p_g = 2.5\times10^6 \text{ Pa in } \Omega_2.$$

Due to the boundary conditions the solution of system is then expected to evolve from this initial condition out of equilibrium state towards a stationary state.

We compare our results to four contributions. The four works have used the same formulation by using the Henry's law to the solvability reaction. In [18] and in [1] the authors use the same primary variables two of the three pressures and recover the thermodynamically extended phase saturation from the retention curve. In [15] the authors formulate the solubility conditions as complementary conditions. Our results named HELMOD are the results obtained by the model HELMOD with the numerical scheme presented in [19]. The results presented as DYNMOD are the only results using the non-equilibrium and approximated in this paper. All numerical tests are obtained with time step $\delta t = 10^{-2}s$ and space step $\delta x = 10^{-2}m$.

Figure 3 shows the evolution of liquid saturation, liquid pressure and dissolved hydrogen density. This figure illustrates the efficiency of our scheme since all quantities reach a stationary state.

Figures 4, 5, 6, 7 give a comparison between five works at $t = 10s$, $t = 50{,}000s$, $t = 200{,}000s$ and $t = 500{,}000s$. All results obtained in the different contributions seem very close and show similar trends.

From Figure 4 to figure 7 we observe the gas flowing in the reverse direction of the physical direction, for the earlier times, resulting from the high gas pressure in the unsaturated zone of the porous medium. That induces a compression of the liquid phase at the left interface, and liberates more space of the water at the opposite side of the domain promoting a decrease of the pressure in that area. One also notices

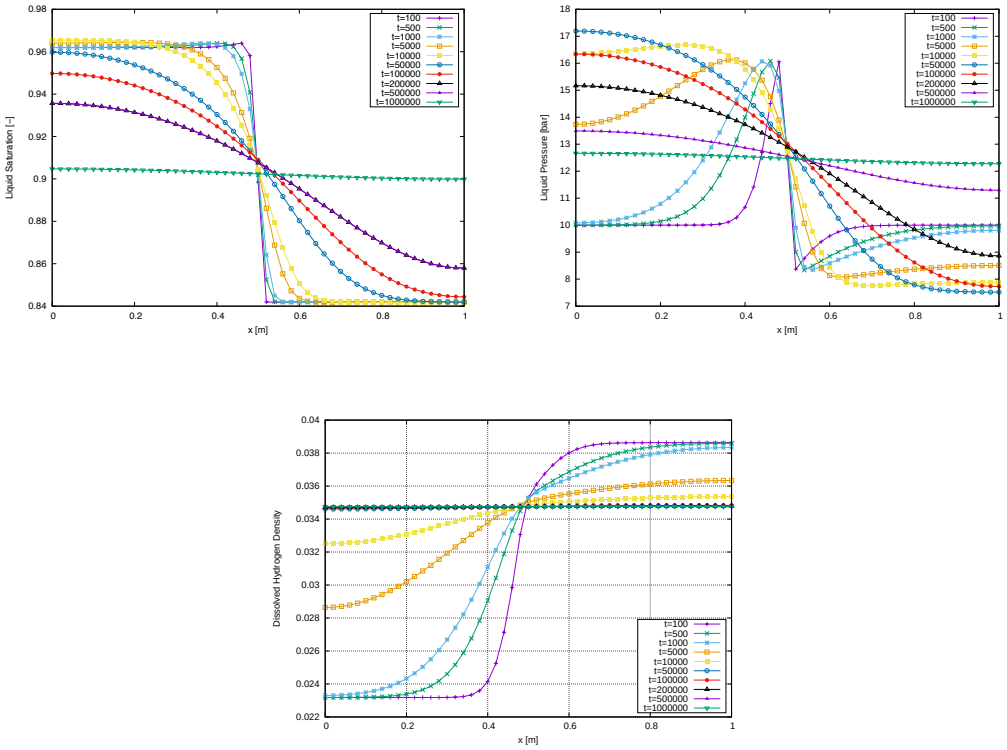

Figure 3: Liquid saturation, liquid pressure and density of dissolved hydrogen at different time with DYNMOD model

also a continuous propagation of the shock up to the pressure equilibrium, that subsequently converges the global system to the equilibrium state. The main difference between the first and the rest of the test cases is the reaching time of the equilibrium.

Acknowledgment. The authors would like to recognize the support of College of Petroleum Engineering and Geosciences, King Fahd University of Petroleum and Minerals (KFUPM).

References

[1] O. Angelini, C. Chavant, E. Chénier, R. Eymard and S. Granet, Finite Volume Approximation of a diffusion-dissolution model and application to nuclear waste storage. Mathematics & Computers in simulation. 81 (2011), 2001–2017.

[2] Bendahmane M., Khalil Z., Saad M., Convergence of a finite volume scheme for gas-water flow in a multi-dimensional porous medium. M3AS Math. Models Methods Appl. Sci. Vol. 24, No. 01, pp. 145–185 (2014).

[3] Bourgeat A., Jurak M., and Smai F., Two-phase, partially miscible flow and transport modeling in porous media; application to gaz migration in a nuclear waste repository. Computational Geosciences, 4(6):309–325, 2009.

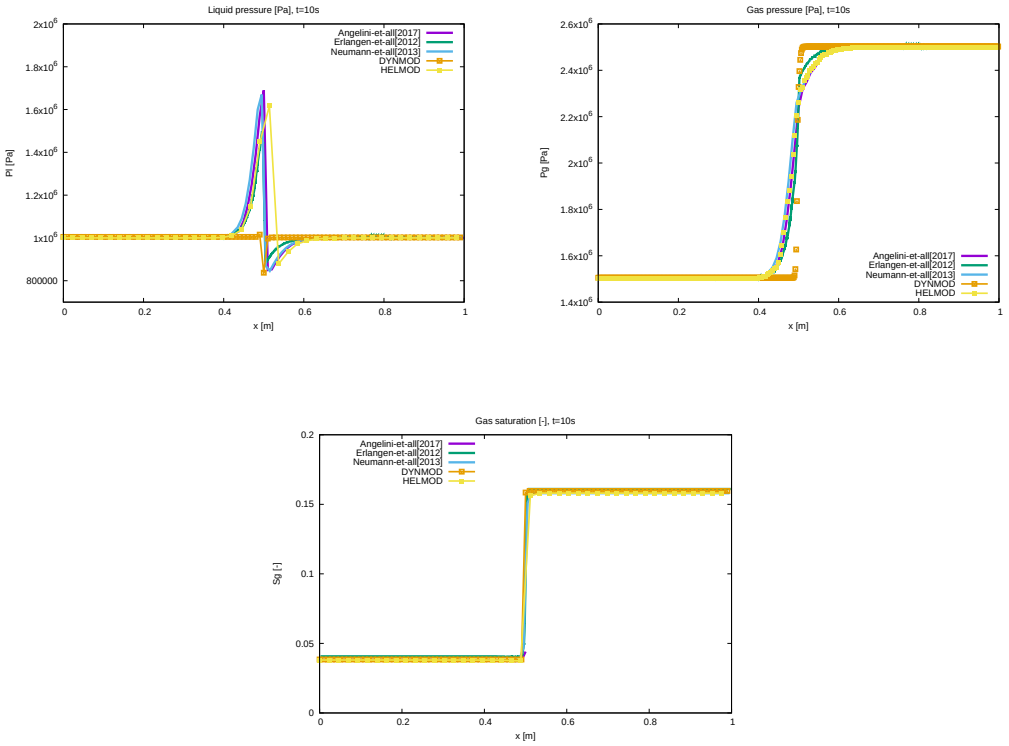

Figure 4: Benchmark test. Comparaison between DYNMOD model and four equilibrium models at time T=10s

[4] Bourgeat, A., Granet, S., Smaï, F., Compositional two-phase flow in saturated-unsaturated porous media: benchmarks for phase appearance/disappearance. Simulation of flow in porous media, 12, 81-106, 2013.

[5] Cai Z., On the finite volume element method, Numerische Mathematik, 1990, 58, 713–735, 1.

[6] F. Caro and B. Saad and M. Saad, *Two-component two-compressible flow in a porous medium*, Acta Applicandae Mathematicae (2012), 117: 15-46,

[7] R. Eymard and T. Gallouët and R. Herbin., *Finite Volume Methods*, Handbook of Numerical Analysis, P. Ciarlet, J. L. Lions, eds, North-Holland, Amsterdam, **7**, pp. 713–1020, 2000.

[8] R. Eymard and R. Herbin and A. Michel, *Mathematical study of a petroleum-engineering scheme*, Mathematical Modelling and Numerical Analysis, **37**, 6, pp. 937–972,

[9] B. Flemisch, M. Darcis, K. Erbertseder, B. Faigle, A. Lauser, K. Mosthaf, S. Muthing, P. Nuske, A. Tatomir, M. Wolff and R. Helmig, DuMux : DUNE for Multi-Phase, Component, Scale, Physics. Advances in Water Resources. 34(9), (2011), 1102–1112.

[10] Z. Khalil and M. Saad, On a fully nonlinear degenerate parabolic system modeling immiscible gas-water displacement in porous media, Nonlinear Analysis, **12**, pp. 1591-1615, 2011.

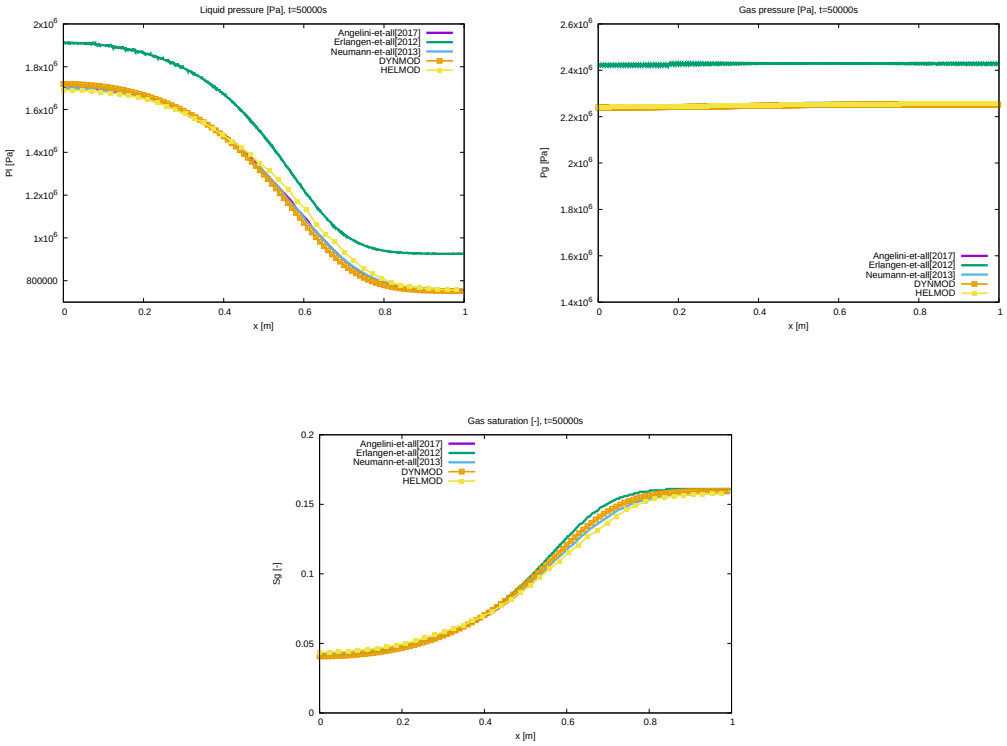

Figure 5: Benchmark test. Comparaison between DYNMOD model and four equilibrium models at time T=50000s

[11] Fabrie P., Le Thiez P., Tardy P., On a system of nonlinear elliptic and degenerate parabolic equations describing compositional water-oil flows in porous media., Nonlinear Analysis:TMA, **28**, 9, 1997, 1565 - 1600

[12] M. Quintard, S. Whitaker, Convection, dispersion, and interfacial transport of contaminants: Homogeneous porous media, Advances in Water Resources, Vol. 17, no. 4, pp. 221-239, 1994.

[13] L. M. Abriola, K. M. Rathfelder and J. R. Lang, Mathematical modeling of rate limited transport and biotransformation in the vadose zone, Comp. Mech. Publications, 136–144, 1996.

[14] A. C. Lam, R. S. Schechter and W. H. Wade, Mobilization of residual oil under equilibrium and nonequilibrium conditions, Society of Petroleum Engineers Journal, vol. 23, 781-790, 1983.

[15] E. Marchand, T. Muller and P. Knabner, Fully coupled generalised hybrid-mixed finite element approximation of two-phase two-component flow in porous media. part II : nu- merical scheme and numerical results, Comp. Geosciences.16, Number 3, (2012), 691–708.

[16] A. Mikelić, A global existence result for the equations describing unsaturated flow in porous media with dynamic capillary pressure. J. Differ. Equ. 248(6), 1561–1577 (2010).

[17] MOMAS, `http://www.gdrmomas.org`,

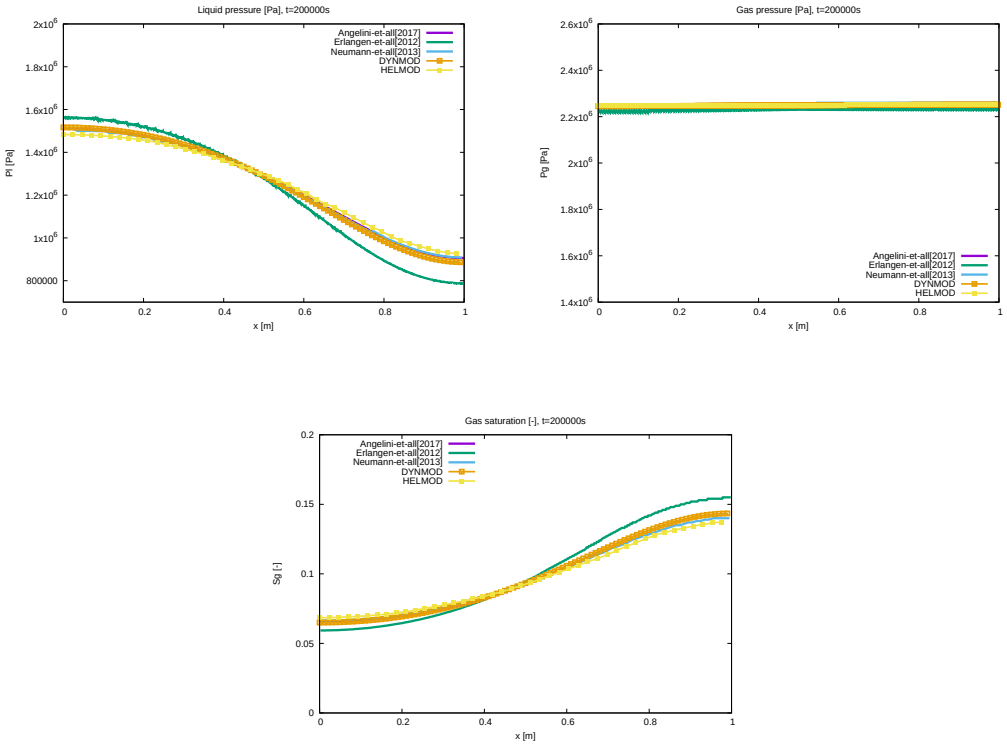

Figure 6: Benchmark test. Comparaison between DYNMOD model and four equilibrium models at time T=200000s

[18] Neumann R., Bastian P. and Ippisch O., Modeling and simulation of two-phase two-component flow with disappearing nonwetting phase, Comput Geosci., 2013, 17, 139-149.

[19] A.S. Saad, B. Saad, M. Saad, Numerical study of compositional compressible degenerate two-phase flow in saturated-unsaturated heterogeneous porous media. *Computers & Mathematics with Applications*, Volume 71, Issue 2, January 2016, Pages 565–584.

[20] B. Saad, M. Saad, Study of full implicit petroleum engineering finite volume scheme for compressible two phase flow in porous media, SIAM J. Numer. Anal., 51(1), 716–741, 2013

[21] B. Saad, M. Saad, Numerical analysis of a non equilibrium two-component two-compressible flow in porous media, Discrete and Continuous Dynamical Systems Series S (DCDS-S), Volume **7**, Number **2**, pp. 317–346, April 2014,

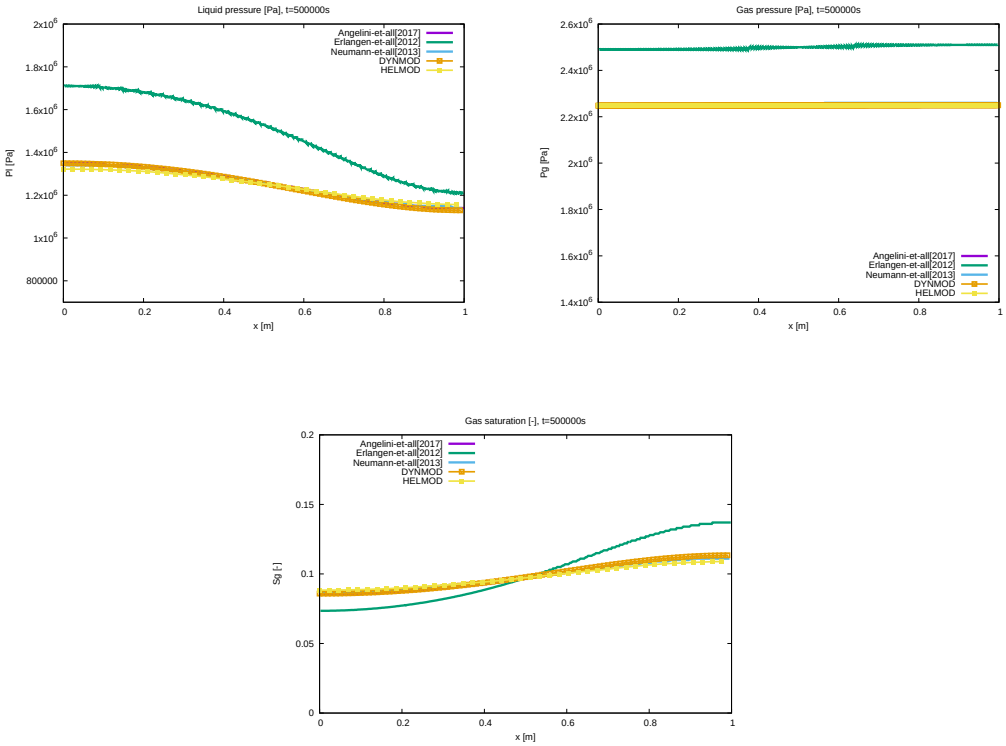

Figure 7: Benchmark test. Comparaison between DYNMOD model and four equilibrium models at time T=500000s